2025 7th International Conference on Control Systems, Mathematical Modeling, Automation and Energy Efficiency (SUMMA) | 979-8-3315-7891-6/25/$31.00 ©2025 IEEE | DOI: 10.1109/SUMMA68668.2025.11302341

Comparative Analysis of Robust Strategies for an Electro-hydraulic Servo Valve System

Aws M. Abdullah
University of Baghdad
Baghdad, Iraq
aws.abd@cois.uobaghdad.edu.iq

Najat Ali Mohammed
University of Baghdad
Baghdad, Iraq
najatali@cois.uobaghdad.edu.iq

Raghad Jamal Munaf
University of Baghdad
Baghdad, Iraq
dr.raghad@rashc.uobaghdad.edu.iq

Nasir Ahmed Alawad
Ashur University
Baghdad, Iraq
nasir.ahmed@au.edu.iq

***Abstract*—PID (proportional-integral-derivative) and Mu controllers are widely used in electro-hydraulic servo systems due to their effectiveness and ease of implementation. This paper explores using particle swarm optimization (PSO) for tuning traditional and robust PID controllers, along with D-K iteration for Mu controller tuning. Three controller types: conventional PID (CPID), robust PID (RPID), and structured singular value controllers are developed, while analyzing multiplicative uncertainty with six uncertain coefficients. Their findings indicated that both PID (CPID and RPID) and Mu controllers maintained system stability. Notably, the Mu controller can handle coefficient uncertainty without a pure integral term, while the RPID controller demonstrated superior performance and reliability. Ultimately, both RPID and Mu controllers provide effective solutions for optimal performance, outperforming CPID in terms of robustness**

Keywords—PID Controller, Mu controller, Particle Swarm Optimization, D-K iteration, Electro-hydraulic Servo Valve System, style, styling, insert

I. INTRODUCTION

The hydraulic servo valve system is crucial in industry due to its high power, fast response time, and lightweight design [1]. The hydraulic servo valve system is complex and nonlinear, making it challenging to control with a linear controller. It often exhibits strong swinging responses. To mitigate this, PID controller tuning methods (CPID and RPID) have been applied, ensuring stability and performance amid varying operating conditions and disturbances [2,3]. PID and Mu-controllers are effective options for system control. PID controllers improve performance under uncertainty, enhance stability, and are versatile, requiring fewer adjustments and sensors while enabling quicker response times. Mu-controllers provide robustness against uncertainties, better performance in multi-input/output systems, ensure stability, and are scalable with a clear design process.

Various studies have examined the use of strong controllers in hydraulic systems [4]. This paper presents a robust control system for electrohydraulic power steering utilizing a 6th-order μ-controller. It demonstrates the system's stability and effectiveness under various conditions, with results indicating reliable performance even amid 25% greater uncertainty than anticipated. Reference [5] outlines the design of a depth controller for a small autonomous underwater vehicle (AUV) using the Mu-synthesis method, addressing performance uncertainties. The study assumes instant fin response, no underwater currents, and no sensor noise. Researchers in [6] assessed a controller's performance and stability through structured singular value Mu-synthesis. They designed a PID controller for a single-input single-output (SISO) system by optimizing the closed-loop poles to achieve the desired performance. They compared its performance with the D-K iteration method, a standard for Mu-synthesis. The paper [7] presented an early V&V μ analysis of the Vega launcher, showing successful comparisons with Monte Carlo methods and optimization tools. Vega is a lightweight launch vehicle developed by the European Space Agency, with ELV S.P.A. as the main contractor. Reference [8] introduced a method for estimating structured singular values (Mu values), which are crucial for assessing the stability of uncertain linear control systems and how system changes impact eigenvalues. Researchers of [9] designed a speed control system for a hydraulic motor using a throttling valve and a constant-displacement pump. They modeled the system's performance in open-loop and feedback scenarios, exploring CPID and H-infinity controllers with a focus on the frequency domain. They also considered variability in system performance and evaluated the system's robustness, comparing time responses in both cases. The work of [10] proposes a reliable and strong PID controller that can handle sensor and actuator failures in the helicopter's TRMS (Tilt Rotor Management System). It features a robust PID controller combined with an $H\infty$ observer, enhancing its reliability. The researchers [11] designed a robust PID controller to manage an electro-hydraulic actuator. This controller accurately positions the actuator piston, even in the presence of various physical uncertainties and external disturbances. I used simulations to demonstrate the actuator's performance.

Researchers of [12] developed a robust control strategy for hydraulic servo actuators using MATLAB/Simulink to manage disturbances that may affect the closed-loop system's operation. The study [13] explores the creation of a control system using the H2 and $H\infty$ control techniques. Results indicate that the $H\infty$ controller maintains system stability, while the H2 controller targets desired performance. In [14], the design of a swing leg system using $H\infty$ loop shaping for robust control is discussed. This system maintains stability and tracking accuracy despite a 20% change in parameters, effectively handling model variations and disruptions. Researchers in [15] developed $H\infty$ and H2 controllers to improve the performance of hydraulic machines. They used the MATLAB/Simulink Toolbox to design and simulate the operation of a hydraulic tire changer machine. The study in [16] examines the certainty in inflow measurement in the Velocity Control System (VCS). It proposed using proportional integral derivative (PID) and $H\infty$ control methods, finding that both perform similarly, but $H\infty$ offers

better robustness. In this research, the speed response of the hydraulic actuator is controlled by input voltage. We analyzed the stability and effectiveness of the system in closed-loop scenarios, designing robust PID and μ-controllers. The paper compares time responses across different scenarios and includes a system model, dynamics analysis with and without uncertainties, and robust controller design along with results and conclusions The formatter will need to create these components, incorporating the applicable criteria that follow.

II. Descrption of the System

The electro-hydraulic servo valve precisely controls the flow of hydraulic fluid to actuators, such as cylinders or motors, based on an electrical signal. It manages hydraulic power by adjusting the position, speed, pressure, or force of the actuator.

Inside the valve, a spool regulates fluid flow by opening and closing ports, with a feedback mechanism monitoring the spool's position. This "closed-loop" system enables continuous adjustments for accuracy. Servo valves typically feature a "zero-lapped" spool design, allowing for immediate and linear responses to small changes in the electrical signal.

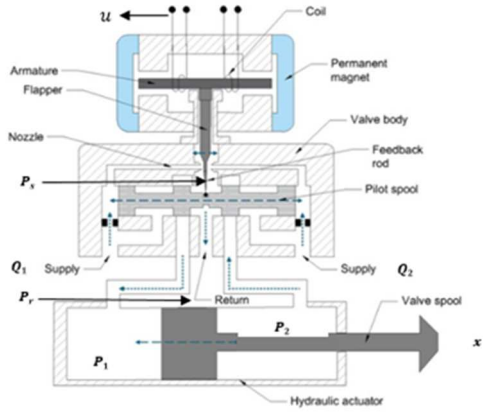

Electro-hydraulic servo valve system

III. Model Stability Analysis

A mathematical model of the electro-hydraulic actuator system will be developed to analyze its responses and address dynamic issues, focusing on the electro-hydraulic servo system. Figure 1 illustrates the actuator's basic components. The cylinder's dynamical model can be described using Newton's Law, as shown in Eq. (1):

$$m\ddot{x} = P_L A - b\dot{x} + kx \tag{1}$$

The actuator displacement is x, and the load mass is m. The total load pressure in the cylinder, P_L, equals the sum of pressures P_1 and P_2 in chambers 1 and 2. The ram area is A, b is the viscous damping coefficient, and k is the spring constant. The load pressure can be expressed with the following equation:

$$\frac{V}{4\beta}\dot{P}_L = -A\dot{x} - CP_L + Q_L \tag{2}$$

The total volume of the cylinder (V) includes the hoses connecting it to the servo valve. β represents the effective bulk modulus, C indicates internal leakage due to pressure, and Q_L $(Q_1 + Q_2) / 2$ is the load flow. Q_L is related to the spool valve movement of the servo valve, as shown in Equation (3):

$$Q_L = c_d w x_v \sqrt{\frac{P_s - sgn(x_v)P_L}{\rho}} \tag{3}$$

The discharge coefficient is c_d, the pilot spool valve area gradient is w, and the fluid supply pressure is P_L with density ρ. The servo valve spool displacement is x_v, and its dynamics are described in Equation (4).

$$\tau_v \dot{x}_v = -x_v + K_v u \tag{4}$$

The spool valve displacement (x_v) is linked to the flapper's current input (u). The parameters τ_v and K_v denote the time constant and gain of the servo-valve, respectively. This work excludes spool dynamics, leading to Equation (5).

$$x_v = K_v u \tag{5}$$

To write the mathematical model of the electro-hydraulic actuator in state space form, we will define the following state variables as shown in Equation (6).

$$\left.\begin{aligned} x_1 &= x \\ x_2 &= \dot{x} \\ x_3 &= P_L \\ u_o &= \sqrt{P_s - sgn(K_v u)x_3}\, u \end{aligned}\right\} \tag{6}$$

We can express the nonlinear mathematical model using the equation labeled as (7):

$$\frac{V}{4\beta}\dot{P}_L = -A\dot{x} - CP_L + Q_L \tag{7}$$

$$Q_L = c_d w x_v \sqrt{\frac{P_s - sgn(x_v)P_L}{\rho}} \tag{8}$$

$$\left.\begin{aligned} \dot{x}_1 &= x_2 \\ \dot{x}_2 &= -\frac{k}{m}x_1 - \frac{b}{m}x_2 - \frac{A}{m}x_3 \\ \dot{x}_3 &= -\frac{4\beta A}{V}x_2 - \frac{4\beta C}{V}x_3 - \frac{4\beta C_d w K_v}{V\sqrt{\rho}}\sqrt{P_s - sgn(K_v u)x_3}\, u \end{aligned}\right\} \tag{9}$$

The term u_0 refers to a new control signal. Since we know that $sgn(u_0)$ matches $sgn(u)$, we can now calculate the actual control, which is the current, using the following relation:

$$u = \frac{u_o}{\sqrt{P_s - sgn(u_o)x_3}}.$$

The control signal u_0 makes the state space model in Eq. (6) a better choice for designing a controller, as we will explain in the next section. The equation for the pressure rise rate is written as:

$$\dot{x}_3 = -\frac{4\beta A}{V}x_2 - \frac{4\beta C}{V}x_3 - \frac{4\beta C_d w K_v}{V\sqrt{\rho}}\sqrt{P_s - sgn(K_v u)x_3}\, u \tag{10}$$

The linearized equation (10) shows the simplified version of the pressure rise rate equation.

$$\dot{x}_3 = -\frac{4\beta A}{V}x_2 - \frac{4\beta C}{V}x_3 - \frac{4\beta C_d w K_v}{V\sqrt{\rho}}\sqrt{P_s}\, u \tag{11}$$

We will define the state variables for the electro-hydraulic actuator in a mathematical model using state space form. This is explained in Eq. (6).

$$\left.\begin{aligned} \dot{x}_1 &= x_2 \\ \dot{x}_2 &= -\frac{k}{m}x_1 - \frac{b}{m}x_2 - \frac{A}{m}x_3 \\ \dot{x}_3 &= -\frac{4\beta A}{V}x_2 - \frac{4\beta C}{V}x_3 - \frac{4\beta C_d w K_v}{V\sqrt{\rho}}\sqrt{P_s}\,u \\ y &= x_2 \end{aligned}\right\} \quad (12)$$

$$A = \begin{bmatrix} 0 & 1 & 0 \\ -\frac{k}{m} & -\frac{b}{m} & -\frac{A}{m} \\ 0 & -\frac{4\beta A}{V} & -\frac{4\beta C}{V} \end{bmatrix} \quad B = \begin{bmatrix} 0 \\ 0 \\ -\frac{4\beta C_d w K_v}{V\sqrt{\rho}}\sqrt{P_s} \end{bmatrix} \quad D = \begin{bmatrix} 0 \\ 0 \\ 0 \end{bmatrix} \quad C = [1 \quad 0 \quad 0] \quad (13)$$

The dynamics of the system were impacted by a response delay; nonetheless, the Routh–Hurwitz stability criterion showed that the open-loop system remains stable [17]. The mathematical model was transformed into transfer functions to demonstrate the connection between input voltage and the area of the valve opening.

$$G(s) = \frac{D_a}{V_{in}} = \frac{25.28s^2+22.2s+3}{s^5+16.6s^4+25.41s^3+17.2s^2+12s+1} \quad (14)$$

let $a_1 = 16.6$, $a_2 = 25.41$, $a_3 = 17.2$, $a_4 = 12$ and $a_5 = 1$

$b_0 = 0$, $b_1 = 0$, $b_2 = 0$, $b_3 = 25.28$, $b_4 = 22.2$ and $b_5 = 3$

IV. Dynamic System Analysis and Controller Design

Robust controllers are designed to handle uncertainties in a system, such as variations in coefficients and external disturbances, while ensuring stability and performance. This is crucial in real-world applications where precise models are often unattainable. The synthesis of robust controllers uses optimization techniques to develop their transfer function. As illustrated in Figure 2, robust controllers rely on the robust controller norm, which maps external signals (reference signals, disturbances, and uncertainties) to controlled outputs. The objective is to minimize this norm [18,19]. Here, C(s) represents the actual output, E(s) is the error signal, and U(s) is the control input.

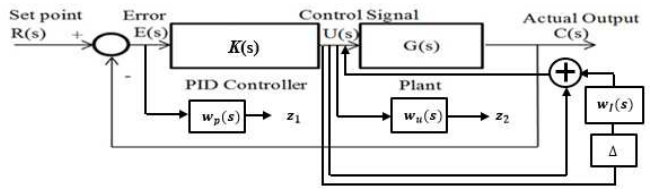

Fig. 2. The schematic representation of the suggested system components along with their corresponding weights

The sensitivity (S) assesses the impact of the reference signal (R) on the error signal (E). This relationship can be described using the formula in Eq. (15).

$$S(s) = \frac{E(s)}{R(s)} = \frac{1}{1+G(s)K(s)} \quad (15)$$

The complementary sensitivity function (T) describes the effect of the reference signal (R) on the output signal (D_a), as shown in Eq. (16).

$$T(s) = \frac{D_a(s)}{R(s)} = \frac{K(s)G(s)}{1+K(s)G(s)} \quad (16)$$

where $T(s) + S(s) = 1$

To assess the system's performance, it is essential to analyze the sensitivity transfer function, bandwidth, and error metrics across a range of frequencies. The transfer function of the robust controller must meet specific criteria [18,19]:

$$|S| < \left|\frac{1}{w_P(j\omega)}\right| , \ |S.K| < \left|\frac{1}{w_u(j\omega)}\right| , \qquad \forall\omega \quad (17)$$

The performance weight (w_p) evaluates how effective a control system is at different frequencies. On the other hand, the control effort weight (w_u) gauges the significance of performance characteristics like tracking precision and disturbance handling. This framework aids in reducing the control energy required for performance while ensuring that system states stay within a specified range [20-22]. To investigate multiplicative uncertainty, perturbed plants will be generated using the earlier transfer functions.

The study investigated six variable factors that influence multiplicative uncertainty, with three varying by ±10% and the other three by ±5%. For accurate results, the parameter (w_I) must exceed the largest error in the frequency spectrum (l_I). We calculated the highest multiplicative error using the standard plant ($G(j\omega)$) and its variations ($G_{pert}(j\omega)$), setting up a standard open-loop system with nominal values for the six factors.

1. Adjust the variation reputation for every parameter in the nominal open-loop system $G(j\omega)$ to obtain $G_{pert}(j\omega)$ as demonstrated in Eq. (18).

$$G_{pert}(j\omega) = G(j\omega)(1 + \Delta) \quad (18)$$

where the variation range of Δ is $\pm$ 10% and $\pm$ 5%.

2. Equation (19) shows the model for how plants behave under uncertain conditions. In contrast, Equation (20) presents the uncertainty weight (w_I).

$$l_I(\omega) = \max_{G_{pert} \in \Pi} \left|\frac{G_{pert}(j\omega) - G(j\omega)}{G(j\omega)}\right| \quad (19)$$

$$l_I(\omega) < w_I(j\omega), \qquad \forall\omega \quad (20)$$

Figure 3 shows how the uncertainty in the electro-hydraulic servo valve system changes with varying coefficients and frequencies. The red curve, representing uncertainty weight (w_I) from Eq. (20), shows no uncertainty at low frequency, about 80% uncertainty at medium frequency, and roughly 0.11% uncertainty at high frequency [23,24].

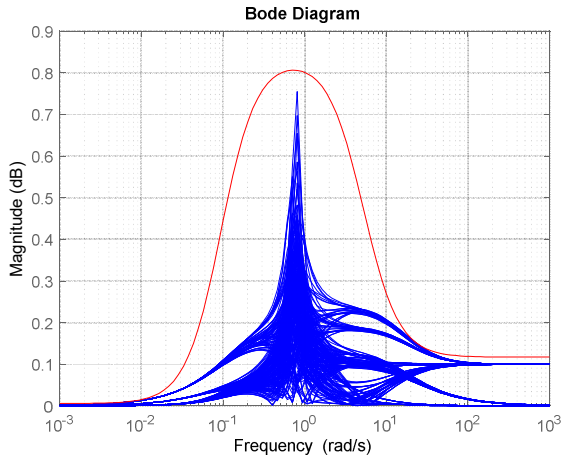

Fig. 3. A transfer function with multiplicative uncertainty constrains the highest potential error.

The uncertainty weight transfer function (w_I) establishes the maximum limit, as described in equations (19) and (20).

$$w_I(s) = \frac{1.014\ s^2 + 5.595s + 0.4953}{s^2 + 5.099s + 0.495} \tag{21}$$

The strong controller transfer function must meet important conditions [82,83]:

$$|T| < \left|\frac{1}{w_I(j\omega)}\right|, \qquad \forall\omega \tag{22}$$

The uncertainty in these equations comes from the stiffness value. This can be expressed as follows:

$$\left.\begin{aligned} b_3 &= b_{3n} + \Delta b_{1n} \\ b_2 &= b_{2n} + \Delta b_{2n} \\ a_1 &= a_{1n} + \Delta a_{1n} \\ a_2 &= a_{2n} + \Delta a_{2n} \\ a_3 &= a_{3n} + \Delta a_{3n} \\ a_4 &= a_{4n} + \Delta a_{4n} \end{aligned}\right\} \tag{23}$$

We can assess the stability of the proposed nonlinear system by considering real-life uncertainties. While the exact values of perturbations are unknown, we often have upper and lower limits. With this information, we can design a robust controller for the perturbed system. The control law function U represents the control voltage supplied to the valve $v_{in}(t)$.

$$V_{in} = K * E \tag{24}$$

$$V_{in}(t) = U \tag{25}$$

In this context, K manages performance, while E represents the difference between the desired speed (R) and actual speed (C) of the actuator.

$$E = R - C \tag{26}$$

You can adjust the control law U to ensure the hydraulic actuator speed matches the desired valve speed despite system uncertainties.

V. The Closed-Loop System That Has Uncertainty

Based on the block diagram shown in Figure 4, we can express the equations for y_Δ, z_1, z_2, and E in the following manner:

$$y_\Delta = u.w_I \tag{27}$$

$$z_1 = -w_P.G.u_\Delta + w_P R - w_P.G.u \tag{28}$$

$$z_2 = u.w_u \tag{29}$$

$$E = -u_\Delta.G + IR - u.G \tag{30}$$

Equations (27–30) are shown in a matrix format, as seen in Equation (23).

$$\begin{bmatrix} y_\Delta \\ z \\ E \end{bmatrix} = [P] \times \begin{bmatrix} u_\Delta \\ \omega \\ u \end{bmatrix} \tag{31}$$

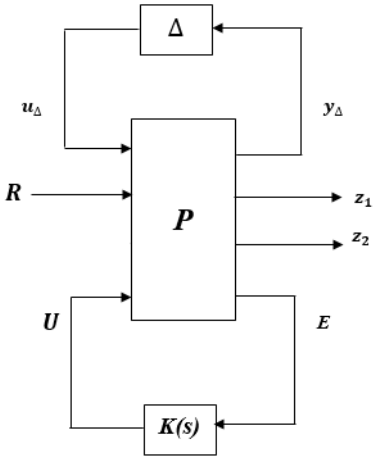

Fig. 4. Schematic representation of the closed-loop system

Equation (32) describes the outside input (ω) and the results (z).

$$\omega = [R] \qquad z = \begin{bmatrix} z_1 \\ z_2 \end{bmatrix} \tag{32}$$

Equation (33) shows the P matrix. Equation (26) lists its parts: P_{11}, P_{12}, P_{21}, and P_{22}.

$$P = \begin{bmatrix} P_{11} & P_{12} \\ P_{21} & P_{22} \end{bmatrix} \tag{33}$$

$$\begin{aligned} P_{11} &= \begin{bmatrix} 0 & 0 \\ -Gw_P & w_P \\ 0 & 0 \end{bmatrix}, \quad P_{12} = \begin{bmatrix} w_I \\ -Gw_P \\ w_u \end{bmatrix}, \\ P_{21} &= [-G \quad 1], \\ P_{22} &= [-G] \end{aligned} \tag{34}$$

In the system matrix (N), shown in Figure 5, the fractional transform can be expressed as follows. [25]:

$$F_L(P,K) = P_{12}.K(I - P_{22}K)^{-1}.P_{21} + P_{11} = N \tag{35}$$

$$F_U\left(\Delta, F_L(K,P)\right) = N_{21}.\Delta.(I - N_{11}.\Delta)^{-1}.N_{12} + N_{22} \tag{36}$$

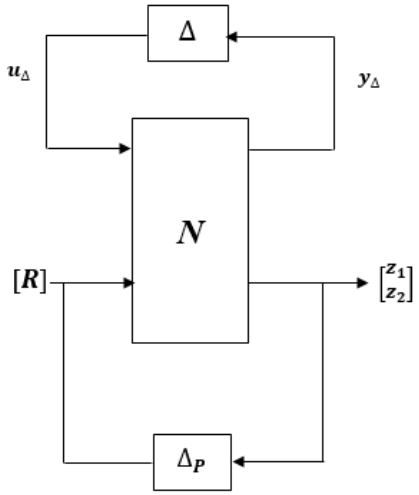

Fig. 5. System nominal block diagram with uncertainty

You can divide an *N* matrix into four parts: N_{11}, N_{12}, N_{21}, and N_{22}. This division is based on performance and stability criteria. [26]:

Nominal Stability (N.S.): The system remains stable despite uncertainties.

Nominal Performance (N.P.): Despite the presence of uncertainties, the system remains stable and fulfills requirements.

$$N.P. \Leftrightarrow \|N_{22}\|_\infty < 1 \tag{37}$$

Robust Stability (R.S.): The system is stable, as shown in Equation (38).

$$R.S. \Leftrightarrow \|N_{11}\|_\infty < 1 \tag{38}$$

Robust performance: The system meets performance goals for all plants affected by uncertainty while ensuring stability, as shown in equation (39):

$$RP \Leftrightarrow \mu(N, \hat{\Delta}) < 1 \tag{39}$$

VI. PID Controller Design

The PID controller enhances the performance and stability of closed-loop systems. Particle Swarm Optimization (PSO) is a technique used to find optimal values for the PID parameters K_p, K_i, and K_d. The Routh-Hurwitz criterion checks for system stability; if it shows instability, the current PSO solution is discarded. The main steps in designing a PSO-based PID controller include:

To establish our cost function, we need to define several key parameters: upper bound *(ub = 100)*, lower bound (*lb = 0*), initial velocity (*v*), population size (*N = 40*), initial position (*x*), maximum inertia weight ($w_{max} = 0.2$), inertia weight (*w*), minimum inertia weight ($w_{min} = 0.7$), and the number of iterations ($T_{max} = 100$).

1. Set initial positions and velocities for the particles.

2. Repeat until stability criteria are met.

3. Use a cost function to calculate the cost for each particle.

4. Revise the best-known cost of each particle (P_{best}) if required.

5. Identify the best overall cost (G_{best}) and update it if needed.

6. Calculate each particle's velocity.

$$v_i = v_i(\tau-1).w + r_1(P_{best,i} - x_i(\tau-1)).\, c_1 + r_2.(G_{best,i} - x_i(\tau-1)).c_2 \tag{40}$$

$$w = w_{max} + \left(\frac{w_{min} - w_{max}}{T_{max}}\right).\, \tau \tag{41}$$

7. Compute the new locations of the particles by:

$$x_i(\tau) = v_i\,(t) + x_i(t-1) \tag{42}$$

8. Stop when you reach the maximum number of iterations or achieve the minimum error limit. If neither condition is met, go back to step 2 [28,29].

VI.I. The Design of the Conventional PID Controller

The classic PID controller was developed under typical plant conditions. Its objective is to reduce the Integral Time of Absolute Error (ITAE), which will serve as the cost function.

$$(\text{ITAE}) = \int_0^t t * |e(t)| dt \tag{43}$$

This study employed Particle Swarm Optimization (PSO) to determine values for the PID controller settings that are close to optimal: K_p=1.5112, K_i=1.0106, and K_d=1.3332. Consequently, the PID controller will be represented as [29]:

$$K(s) = 1.5112 + \frac{1.0106}{s} + 1.3332S \tag{44}$$

VI.II. Robust PID Controller Design

The Robust PID controller was designed based on the main characteristics of the plant while considering any uncertainty. In addition, the cost function calculates the cost for each particle in the swarm [29]:

$$\text{The cost function} = \left\| |W_P S| + |W_I T| \right\|_\infty < 1 \tag{45}$$

where $|W_P S| < 1$, $|W_I T| < 1$,

This study employed Particle Swarm Optimization (PSO) to determine nearly optimal values for the parameters of the PID controller. The outcomes are: $K_d = 3.1$, $K_i = 1.8335$, and $K_p = 0.98$. Consequently, these values will define the Robust PID controller.

$$K(s) = 3.1S + \frac{1.8335}{s} + 0.98\,. \tag{46}$$

The weight of the performance is indicated in Equation (47).

$$w_p = \frac{\frac{S}{M} + \omega_b}{S + a\omega_b} = 0.1\,\frac{S+0.3}{S+0.3\times10^{-4}} \tag{47}$$

The low-frequency error is 0.0001 and the high-frequency error (*M*) is 1, with a bandwidth frequency (ω_b) of 0.3. A gain of 0.1 ensures manageable steady-state error, while the input (w_u) is set to its maximum value and the control effort weight (w_u) is 1.

VII. Mu-Controller Design

The Mu controller uses the μ-value to measure how effectively a control system can manage uncertainties. It indicates the system's sensitivity to changes in specific conditions, requiring you to define the types of uncertainties involved, such as varying coefficients or external influences. When designing the control system, aim to keep the μ-value below a set limit for all defined uncertainties to ensure stability and performance. The LFT represents the system needing control [30,31]:

$$[F_U(F_L(K,P),\Delta),\ max_\omega\ \bar{\sigma}\ [\Delta(j\omega)] \leq 1] \quad (48)$$

The objective is to identify a controller *K* that guarantees the stability of the system while maintaining the highest value $max_\omega\ \bar{\sigma}\ [\Delta(j\omega)] \leq 1$.

We can evaluate any controller *K*'s performance using a robust performance test on the linear fractional transformation *N*, particularly focusing on the uncertain area represented by (Δ_P). The system with controller *K* performs well when the following condition is met.

$$\mu_{\tilde{\Delta}}\big(F_L(P,K)(j\omega)\big) < 1 \quad (49)$$

The goal of μ-synthesis is to minimize the structured singular value $\mu_{\tilde{\Delta}}$ in the closed-loop transfer function by finding all stabilizing controllers *K*.

$$min\ \ max_\omega\ \mu_{\tilde{\Delta}}(F_L(P,K)(j\omega)) \quad (50)$$

The μ-synthesis technique that utilizes D–K iterations consists of these steps:

1. Obtain the model of the uncertainty plant, which includes the components *of the P* matrix: P_{11}, P_{12}, P_{21}, and P_{22}.

2. set $D = I$ (the identity matrix).

3. Maintain *D* and perform the *H*-optimization to determine

$$K = arg\ inf\left\|F_L(K,\tilde{P})\right\|_\infty \quad (51)$$

K
with $P = \begin{bmatrix} D & 0 \\ 0 & I \end{bmatrix} \times P \times \begin{bmatrix} D^{-1} & 0 \\ 0 & I \end{bmatrix}$ well-matched with the partition of *P*

Adjust *D* and resolve the subsequent convex optimization task for *D* at every frequency across a specified range of frequencies.

$$D(j\omega) = arg\ inf\bar{\sigma}[DF_l(K,P)D^{-1}(j\omega)] \quad (52)$$
$$D \in \boldsymbol{D}$$

To create a stable, minimum-phase *D(s),* fit the curve *D(jω)*, then repeat the process until you meet the desired accuracy or criteria in Equation (53), or until reaching the maximum allowed iterations.

$$sup\ \ inf\bar{\sigma}[DF_l(K,P)D^{-1}(j\omega)] \quad (53)$$
$$\omega \in \boldsymbol{\mathcal{R}} \quad D \in \mathbf{D}$$

The D–K iteration method makes effective use of frequency-dependent weighting functions, particularly the control effort weight (w_u) and the performance weight (w_p). The performance weight indicates the system's capacity to fulfill performance objectives and adjusts the output sensitivity function accordingly [32,33], as demonstrated in Equation (54).

$$w_p = \frac{\frac{S}{M}+\omega_b}{S+a\omega_b} = 0.5\,\frac{\frac{S}{4}+0.25}{S+0.25\times10^{-4}} \quad (54)$$

The parameter ω_b is fixed at 0.25, while the high-frequency error is *M=4* and the low-frequency error is *a=0.0001*. We select a gain of *0.5* to maintain a minimal steady-state error, although increasing the gain may lead to a slower system response. The weighting control function (w_u) constrains the controller gain and balances the competing objectives, typically set to one based on maximum value normalization, as illustrated in Figure 2. [34,35].

The transfer function of the Mu-controller was estimated using the MATLAB function dksyn.m, as shown in Eq. (55).

$$K(s) = \frac{0.8148\,s^6 + 2.071s^5 + 2.964\,s^4 + 1.95\,s^3 + 1.208s^2 + 0.2071s + 0.01026}{s^7 + 8.619\,s^6 + 22.83\,s^5 + 31.32s^4 + 18.4s^3 + 3.358s^2 + 0.1792s + 4.479e{-}06} \quad (55)$$

The M-file commands are used for Mu-synthesis to find an effective controller with an optimal μ value of 0.9342. The command (dksyn.m) analyzes the system's closed-loop μ with a stable M-Controller, ensuring strong stability and performance.

VIII. Analysis of the Results

Figure 6-7 illustrates the performance of closed-loop systems with and without robust controllers. Starting at a target position of *8* mm, robust controllers enhance stability and aid the actuator in achieving the desired speed. In contrast, the CPID controller struggles with oscillations and overshooting, while the RPID and Mu controllers perform better and are more reliable. Table 1 summarizes the compression results for all robust controllers.

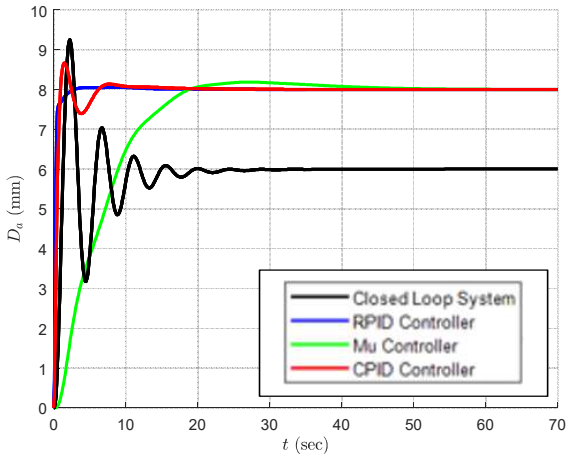

Fig. 6. The position response (upward movement) of the hydraulic actuator over time for the closed-loop system, both without and with the implementation of all robust controllers in the presence.

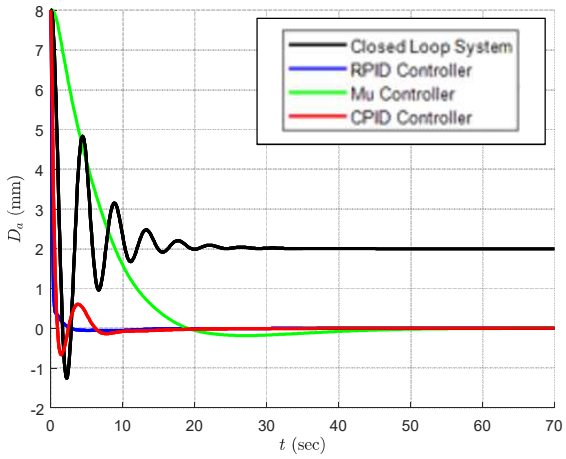

Fig. 7. The position response (downward movement) of the hydraulic actuator over time for the closed-loop system, both without and with the implementation of all robust controllers in the given context.

TABLE I. OUTCOMES OF THE POSITION TIME RESPONSE FOR HYDRAULIC ACTUATORS UTILIZING ROBUST CONTROLLERS

Robust Controllers	Closed loop	CPID	RPID	Mu
Rise time	1.64 sec	0.9 sec	0.3513 sec	19.21 sec
Steady state value	18 sec	8 sec	2 sec	26 sec
Max. overshoot	15.675 %	8.29 %	0	2.25 %
Steady state error	0.2 m/s	0 m/s	0 m/s	0 m/s

The control action voltage for a closed-loop system with strong controllers is shown in Figure 8, indicating similar voltage levels that stabilize at a final value. Table 2 presents the compression results for all the strong controllers.

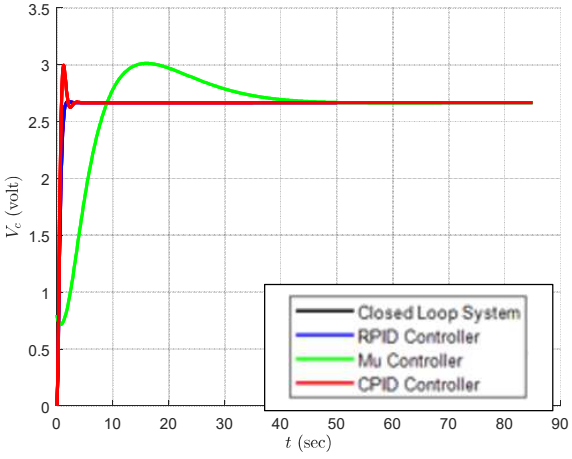

Fig. 8. Response over time of the control action for closed-loop systems utilizing robust controllers

TABLE II. OUTCOMES OF RESPONSE TIME FOR CONTROL ACTIONS USING ROBUST CONTROLLERS

Robust Controllers	**CPID**	**RPID**	**Mu**
Steady state value	2.472 sec	1.45 sec	8.565 sec
Rise time	1.686 sec	0.816 sec	8.901 sec
Max. overshoot	12.53 %	0.9377 %	12.53 %

Figure 9 illustrates the response of the uncertain system over time under conditions of multiplicative uncertainty. The time response of the closed-loop system is comparable for each controller, even as the uncertainties fluctuate. To assess these uncertainties, we examined the errors in the nominal system's uncertain coefficients, which varied between ±10% and ±5% of their nominal values. Our analysis revealed that both the PID (CPID and RPID) controllers and the Mu-controller exhibited similar response levels despite these uncertainties. Importantly, the answers showed considerable stability and exceptional performance, even when faced with substantial uncertainties.

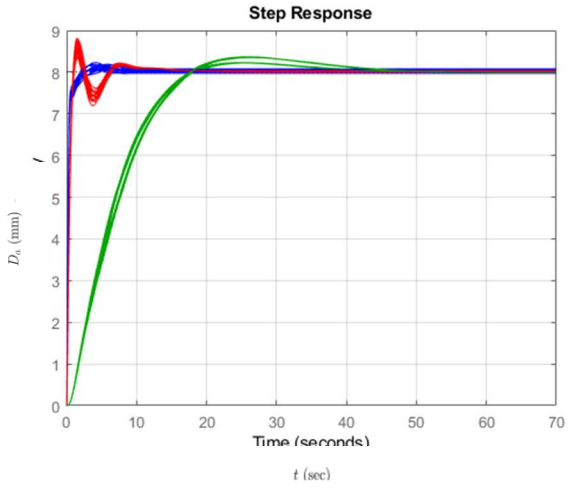

Fig. 9. The reaction time of the disturbed hydraulic actuator speed for the closed-loop system utilizing all robust controllers.

Figure 10 indicates that the CPID, RPID, and Mu controllers are stable, with all values of $\|N_{11}\|_\infty$ below 1, peaking at 0.9049, 0.7653, and 0.7117 within the (10^{-3} - 10^{3}) range. In Figure 11, each controller achieves nominal performance, with maximum values of 0.8399, 0.8455, and 0.8593. However, only the RPID and Mu controllers satisfy the robust performance condition, $\mu_{\hat{\Delta}}$, reaching maximums of about 0.9967 and 0.9342 in Figure 12.

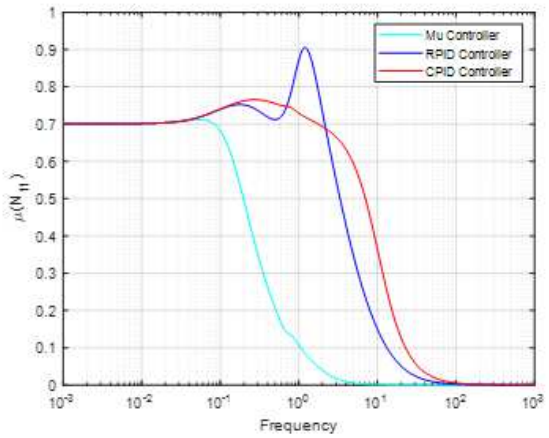

Fig. 10. The criteria for ensuring robust stability.

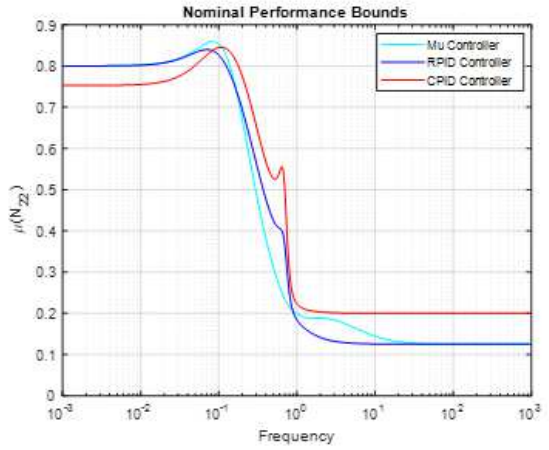

Fig. 11. The criteria for the standard performance.

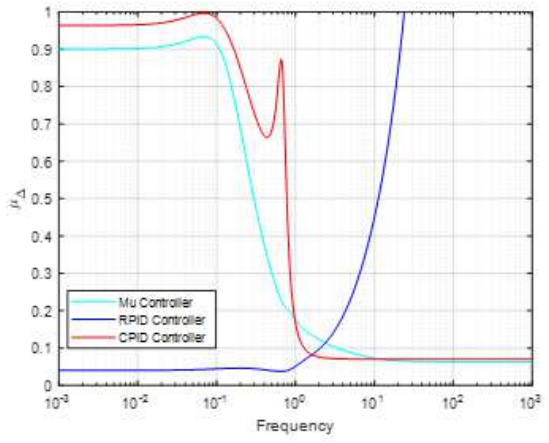

Fig. 12. The necessity for strong performance.

CONCLOSSIONS

We tested the electro-hydraulic servo valve system both independently and with robust controllers. The results indicate our model exhibits minimal tracking error and stability. Key points include:

- The electro-hydraulic servo valve system is efficient and cost-effective for flow control, but closed-loop speed control shows large steady-state errors and struggles with disturbances. In contrast, systems with robust controllers perform better, using less power and improving efficiency.
- With robust controllers, the closed-loop system responds faster, displaying small steady-state errors, effective disturbance handling, and fewer oscillations, particularly with CPID controllers, which also enhance stability.
- Simulation results demonstrate that the Mu and RPID controllers meet stability and performance goals. The RPID and Mu controllers reduce overshoot, with the Mu controller avoiding oscillations by not having a pure integral term, while CPID controllers often cause overshoot and oscillations.

NOMENCLATURE

b Viscous damping coefficient, m/s

A Ram area of the cylinder, m^2

V Total volume of the cylinder and the hoses between the cylinder and the servo valve, m^3

C Coefficient of the total internal leakage of the cylinder due to pressure, m^5/Ns

k Effective bulk modulus of spring, N/m

C_d Discharge coefficient

w Spool valve area gradient, m^2

m Mass of the load, kg

Ps Supply pressure of the fluid, N/m^2

k_v Gain of the servo-valve

GREEK SYMBOLS

β Effective bulk modulus of spring, N/m^2

ρ Fluid density, kg/m^3

REFERENCES

[1] N. D. Manring," Mapping the Efficiency for a Hydrostatic Transmission," Journal of Dynamic Systems, Measurement, and Control MARCH 2016, Vol. 138 / 031004-1 Copyright V.C. 2016 by ASME.

[2] Z. Jing and H. Qi," Design and Calculation of Hydraulic Transmission System of Loader," MMEAT 2020 Journal of Physics: Conference Series 1676 (2020) 012242 IOP Publishing, doi:10.1088/1742-6596/1676/1/012242.

[3] H. H. Ali, and R. C. Fales," A review of flow control methods," International Journal of Dynamics and Control (2021) 9:1847–1854 https://doi.org/10.1007/s40435-020-00730-y.

[4] J. Kralev, A. Mitov, I. Angelov and T. Slavov " Robust Mu-Controller for Electro-Hydraulic Steering System ", 978-1-5386-9301-8/19/$31.00 ©2019 European Union

[5] M. Ba Loc, H. Sik Choi, S. Sang You, and T. Woong Um " Mu-synthesis Depth Controller Design for a Small Autonomous Underwater Vehicle," International Symposium on Mechatronics and Robotics, October 26-28, 2011, HCMUT, Vietnam, Conference Paper · January 2011.

[6] N. Guglielmi, M. Ur Rehman and D. Kressner," A Novel Iterative Method to Approximate Structured Singular Values" SIAM J. MATRIX ANAL. APPL. 2017 Society for Industrial and Applied Mathematics, Vol. 38, No. 2, pp. 361–386

[7] A. Marcos, P. Rosa, C. Roux, M. Bartolini and S. Bennani, "An Overview of the RFCS Project V&V Framework: Optimization-Based and Linear Tools for Worst-Case Search," CEAS Space Journal, Vol. 7, No. 2, 2015, pp. 303–318.

[8] N. Guglielmi, M. Ur Rehman and D. Kressner," A Novel Iterative Method to Approximate Structured Singular Values" SIAM J. MATRIX ANAL. APPL. 2017 Society for Industrial and Applied Mathematics, Vol. 38, No. 2, pp. 361–386

[9] a. M. Abdullah, H. H. Ali, A. A. al-qassar, "A Robust Controller Design for an Inlet Throttling Velocity Controller System for A Rotery Actuator", International Journal of Mechatronics and Applied Mechanics, 2024, Issue 15.

[10] V. Rao, S. Kamath, V. I. George, and S. C " Reliable Robust PID Controller Design for TRMS " Conference Paper .December 2017

[11] M. G. Skarpetis, F. N. Koumboulis," Robust PID Controller for Electro - Hydraulic Actuators ", 978-1-4799-0864-6/13/$31.00 ©2013 IEEE.

[12] Z. Gosiewski and M. Henzel," A Robust Controller for Electrohydraulic Drives ", Solid State Phenomena Vol. 113 (2006) pp 61-66 Online available since 2006/Jun/15 at www.scientific.net © (2006) Trans Tech Publications, Switzerland doi:10.4028/www.scientific.net/SSP.113.61

[13] A. J. Ali, H. H. Abbas and H. Bevrani," Comparative Analysis of H2 and H∞ Robust Control Design Approaches for Dynamic Control Systems", Volume 29 Number 8 August 2023

[14] S. Sami Ali, S. M. R. and A. Al-Khazraji, " Improving the performance of medical robotic system using H∞ loop shaping robust controller " Int. J. Modelling, Identification and Control, Vol. 34, No. 1, 2020.

[15] M. Msallam , N. Alawad , A. Al Mhdawi , A. Al-Khazraji , S.Husain , A.Huamidi, " ANN-Based Ship Maneuvering Motion Control " 8th IET Smart Cities Symposium (SCS 2024), Hybrid Conference, Bahrain 1–3 December 2024.

[16] H. Ali, R. Fales (2020) "Robust control design for an inlet metering velocity control system of a linear hydraulic actuator." Int J Fluid Power. https://doi.org/10.13052 /ijfp1439-9776.2113.

[17] H. H. Ali., F. M. Abdulsattar, and A. W. Mustafa, "A New MechanicalAnalysis of a Crankshaft-connecting Rod Dynamics Using Lagrange's Trigonometric Identities", Journal of Engineering & Technological Sciences vol.54, no.2, 2022

[18] https://doi.org/10.5614/j.eng.technol.sci.2022.54.2.9

[19] R. G. Orozco, “Mixed Sensitivity Control: A Non-Iterative Approach”, Systems Science & Control Engineering, vol.8, no.1, pages 441-453, 2020. https://doi.org/10.1080/21642583.2020.1793821

[20] N. A. Al-awad, “Optimal Controller Design for Reduced-Order Model of Rotational Mechanical System”, Mathematical Modelling of Engineering Problems, vol.7,No.3,September, pages 395-402, 2020. https://doi.org/10.18280/mmep.070309.

[21] J. K. Wisch, “Dynamic and Efficiency Characteristics of an Inlet Metering Valve Controlled Fixed Displacement Pump”, Ph.D. dissertation, University of Missouri, Columbia, MO, 2016.

[22] L. Dubonji´c, S. Prodanovi´c, V. Stojanovi´c, M.M. Morato, “PD controller design for a system of a valve controlled hydro motor”, Engineering Today, vol.2, no.3, pages 8, 2023. https://doi.org/10.5937/engtoday2300012D

[23] Z. and D., “Essentials of Robust Control”, Prentice-Hall, 1999.

[24] P. Biswas, R. Maiti, A. Kolay, K. D. Sharma, G. Sarkar, “PSO based PID controller design for twin rotor mimo system”, in: Proceedings of The 2014 International Conference on Control, Instrumentation, Energy and Communication (CIEC), IEEE, pages 56-60, 2014. DOI: 10.1109/CIEC.2014.6959049

[25] V. S. Rao, V.I. George, S. Kamath, C. Shreesha, “Reliable H-infinity Observer-Controller Design for Sensor and Actuator Failure in TRMS”, Proceedings ICAEE-2014, VIT Vellore, IEEE Xplorer, 2014. DOI. 10.1109/ICAEE.2014.6838536

[26] K. Puttannaiah, “A Generalized H-infinity Mixed Sensitivity Convex Approach to Multivariable Control Design Subject to Simultaneous Output and Input Loop-Breaking Specifications”, Dissertation Presented in Partial Fulfillment of the Requirements for The Degree Doctor of Philosophy, Arizona State University, 2018.

[27] P. Saini, P. Thakur, “H-Infinity Based Robust Temperature Controller Design for a Non-linear Systems”, Wireless Pers, Commun. 2022, vol.126, pages 305–333, 2022. https://doi.org/10.1007/s11277-022-09746-3

[28] N. Ishak, M. Tajjudin, “Real-time Application of Self-tuning PID in Electro-Hydraulic Actuator”, IEEE International Conference on Control System, Computing and Engineering (ICCSCE), pages 364–368, 2012. DOI: 10.1109/ICCSCE.2011.6190553

[29] S. Chaudhary, A. Kumar, “Control of Twin Rotor MIMO System Using 1-Degree-of-Freedom PID, 2-Degree-of-Freedom PID and Fractional Order PID Controller”, in: 2019 3rd International conference on Electronics, Communication and Aerospace Technology (ICECA), IEEE, pages 746-751, 2019. DOI: 10.1109/ICECA.2019.8821923

[30] Y. Ye, C.B. Yin, Y. Gong, J.J. Zhou, “Position Control of Nonlinear Hydraulic System Using an Improved PSO based PID controller”, Journal of Mechanical Systems and Signal Processing, voL.83, pages 241–259, 2017. https://doi.org/10.1016/j.ymssp.2016.06.010

[31] D. Song, X. Li, Z. Peng, “Mixed Sensitivity H-infinity Control of an Adaptive Optics System”, Optical Engineering vol.55, no.9, 2016. doi: 10.1117/1.OE.55.9.094106

[32] N. Guglielmi, M. Ur Rehman and D. Kressner," A Novel Iterative Method to Approximate Structured Singular Values", SIAM Journal on Matrix AnalysisApplications 2017 (Society for Industrial and Applied Mathematics), vol.38, no.2, pages 361–386, 2017. https://doi.org/10.1137/16M1074977

[33] I. Mehta, V. Garg and R.J. Abraham, “Design of a Robust Controller for a DC Motor with Structured Uncertainties”, International Journal of Dynamics and Control, vol.11, no.2, pages 680–688,2023. Doi:10.1007/s40435-022-01025-0.

[34] V. Fakhari, S. B. Choi, & C. H. Cho, “A New Robust Adaptive Controller for Vibration Control of Active Engine Mount Subjected to Large Uncertainties”, Smart Materials and Structures 2015; vol.24, no.4, 2015. **DOI** 10.1088/0964-1726/24/4/045044

[35] P. Petkov, Ts. Slavov, etc. “Design of Embedded Robust Control Systems using MATLAB®/Simulink®”, The Institution of Engineering and Technology, 2018. DOI: 10.1049/PBCE113E

[36] F. H. Chung, "Machine Learning Techniques for Controller Optimization", Journal of Process Control Engineering, vol. 71, no. 4, pp. 312-322, 2023.

[37] doi: 10.1016/j.jprocont.2023.05.002